Journal of Nuclear Materials 405 (2010) 9–16

Contents lists available at ScienceDirect

Journal of Nuclear Materials

journal homepage: www.elsevier.com/locate/jnucmat

Effects of high temperature aging in an impure helium environment on low temperature embrittlement of Alloy 617 and Haynes 230

Daejong Kim, Injin Sah, Changheui Jang *

Department of Nuclear and Quantum Engineering, KAIST, 335 Gwahangno, Yuseong-gu, Daejeon 305-701, Republic of Korea

ARTICLE INFO

Article history:
Received 8 April 2010
Accepted 20 July 2010

ABSTRACT

The effects of high temperature environmental damage on low temperature embrittlement of wrought nickel-base superalloys, Alloy 617 and Haynes 230 were evaluated. They were aged in an impure helium environment at 1000 °C for up to 500 h before tensile tested at room temperature. The tensile test results showed that the loss of ductility was associated with the increase in the inter-granular fracture with aging time. For Alloy 617, inter-granular oxidation and coarsening of grain boundary carbides contributed to the embrittlement. The significant loss of ductility in Haynes 230 was only observed after 500 h of aging when the globular intermetallic precipitates were extensively formed and brittle inter-granular cracking began to occur.

1. Introduction

Wrought nickel-base superalloys, such as Alloy 617 and Haynes 230 are the materials considered for the intermediate heat exchanger (IHX) applications in a very high temperature gas cooled reactor (VHTR) with an outlet gas temperature of 900 °C and above [1,2]. Based on the operating experience of the earlier high temperature gas cooled reactors, the helium coolant in the primary circuit is likely to contain small amounts of gaseous impurities such as CO, CO_2, CH_4, H_2O and H_2 in operating condition [3,4]. It has been known that the high temperature environmental degradations such as oxidation, decarburization and carburization in the impure helium environment could be extensive depending on temperature and the levels of impurities [5–8]. Such environmental damage can significantly degrade the mechanical properties of the materials for the IHX applications [9], and eventually the life and performance of the components. Especially, carburization and decarburization can result in the low temperature embrittlement and the reduction in creep or creep-fatigue strength [10]. In this study, the low temperature embrittlement behaviors of Alloy 617 and Haynes 230 were investigated to understand the relationship between environment and microstructure, and their effects on the mechanical properties. Specimens were aged in an impure helium environment and subsequently tensile tested at room temperature. The microstructure evolution such as internal oxide growth along grain boundary and coarsening of inter- and intra-granular carbides was discussed in view of their effects on the embrittlement.

* Corresponding author. Tel.: +82 42 350 3824; fax: +82 42 350 3810.
E-mail address: chjang@kaist.ac.kr (C. Jang).

0022-3115/$ - see front matter © 2010 Elsevier B.V. All rights reserved.
doi:10.1016/j.jnucmat.2010.07.026

2. Experimental

Two commercial grade wrought nickel-base superalloys, Alloy 617 and Haynes 230 were used in this study. Chemical compositions of the materials are listed in Table 1 and typical microstructures are shown in Fig. 1. As shown in the figures, the as-received microstructures contain twins, well-distributed primary carbides and grain boundary carbides. Grain boundary carbides were primarily $M_{23}C_6$ type carbides precipitated during solution anneal heat treatment. The small-size plate-type tensile specimens with 0.5 mm in thickness, shown in Fig. 2, were machined and aged at 1000 °C in the impure helium containing 5.0 Pa CO, 1.0 Pa CO_2, <0.1 Pa CH_4, and 0.07 Pa H_2O up to 500 h. During the aging treatment, gas flow rate was maintained at 500 cc/min. Aged specimens were tensile tested at room temperature. For the tested specimens, metallographic analyses were carried out using transmission electron microscopy (TEM), scanning electron microscopy (SEM), and energy dispersive X-ray spectroscopy (EDS).

3. Results and discussion

3.1. Microstructure evolution

Fig. 3 shows the cross-sectional area of Alloy 617 and Haynes 230 aged for 500 h at 1000 °C in the impure helium environments. It is clear from the figures that there are three distinct zones such as an oxidation region, narrow band of the carbide-free zone, and a matrix in which an increased volume fraction of carbides, grain boundary carbides in particular, were observed. Overall, the microstructure evolution during the aging treatment in the impure

Table 1
Chemical composition of Alloy 617 and Haynes 230 (wt.%).

	Cr	Al	C	Co	Fe	Mn	Mo	Ni	Si	Ti	W
Alloy 617	21.6	1.5	.1	11.8	1.14	.05	8.92	Bal.	.5	.35	–
Haynes 230	21.5	.29	.1	.36	2.94	.46	1.09	Bal.	.38	–	13.8

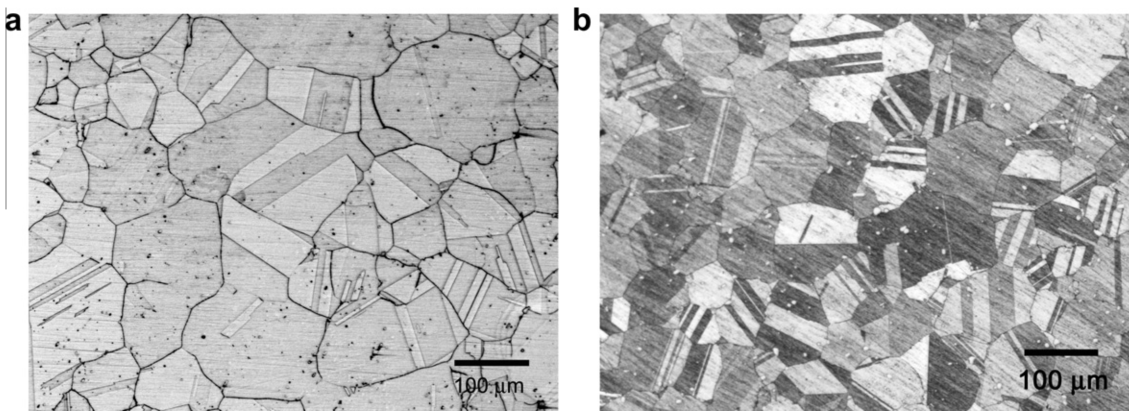

Fig. 1. Typical microstructure of as-received specimens: (a) Alloy 617 and (b) Haynes 230.

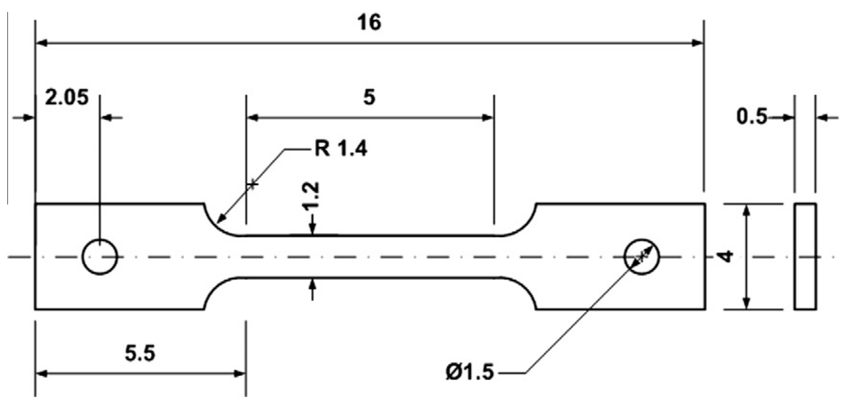

Fig. 2. Geometry of the small-size plate-type tensile specimen.

helium environments seems quite similar to that in air and helium environments [11].

Both alloys were known to be oxidized by CO_2 and H_2O contained in the helium gas by the following reactions [12]:

$$xM + y/2CO_2 \rightarrow M_xO_y + y/2C_{solution} \quad (1)$$

$$xM + yH_2O \rightarrow M_xO_y + y/2H_2 \quad (2)$$

In high temperature helium environments containing small amount of oxidizing impurities, it was reported that the oxide layers were mostly Cr_2O_3 for Alloy 617, and Cr_2O_3 and $MnCr_2O_4$ for Haynes 230 based on the thin-film XRD and SEM/EDS analysis [13]. Below the surface oxide layer, carbides were almost decomposed and the carbide-free zone was formed by the following decarburization reactions [7].

$$2Cr_2O_3 + 6H_2 \rightarrow 6H_2O + 4Cr \quad (3)$$

$$Cr_{23}C_6 \rightarrow 6C_{solution} + 23Cr \quad (4)$$

$$6C_{solution} + H_2O \rightarrow 6CO + 6H_2 \quad (5)$$

The significant coarsening of carbides was observed below the carbide-free zone while oxidation and decarburization happened near the surface. Carbides became more continuous and thicker on grain boundaries for both alloys. Especially for Haynes 230, lots of fine carbides were dispersed within grains and globular carbides were grown as intra- and inter-granular carbides. The supply of carbon for the coarsening of carbides can be induced by several mechanisms. First is the inward diffusion of carbon produced by the dissociation of CO and CH_4 in metal or oxide surface. Second is the inward diffusion of carbon produced during the decarburization process (Eq. (4)). Third is the carbon in the matrix, or 0.1 wt.% for the alloys used.

In this study, very low CH_4 and low CO contents in impure helium would induce the decarburizing condition for Alloy 617 and Haynes 230 and carbon in metal or oxide surface rapidly react with H_2O in impure helium. Therefore, the inward diffusion of carbon into matrix would be very limited [14]. Moreover, carbon produced by the decomposition of carbides during decarburization reacts with H_2O within the matrix (Eq. (5)) and produce CO gas. CO within the matrix was thought to diffuse outward rather than inward based on the study that a carbon concentration decreases as function of time when nickel-base superalloys are decarburized in the simulated VHTR environments [15]. Therefore, the decarburization and the oxidation by CO_2 would not affect the growth of carbides below the carbide-free zone. Nevertheless, the coarsening of car-

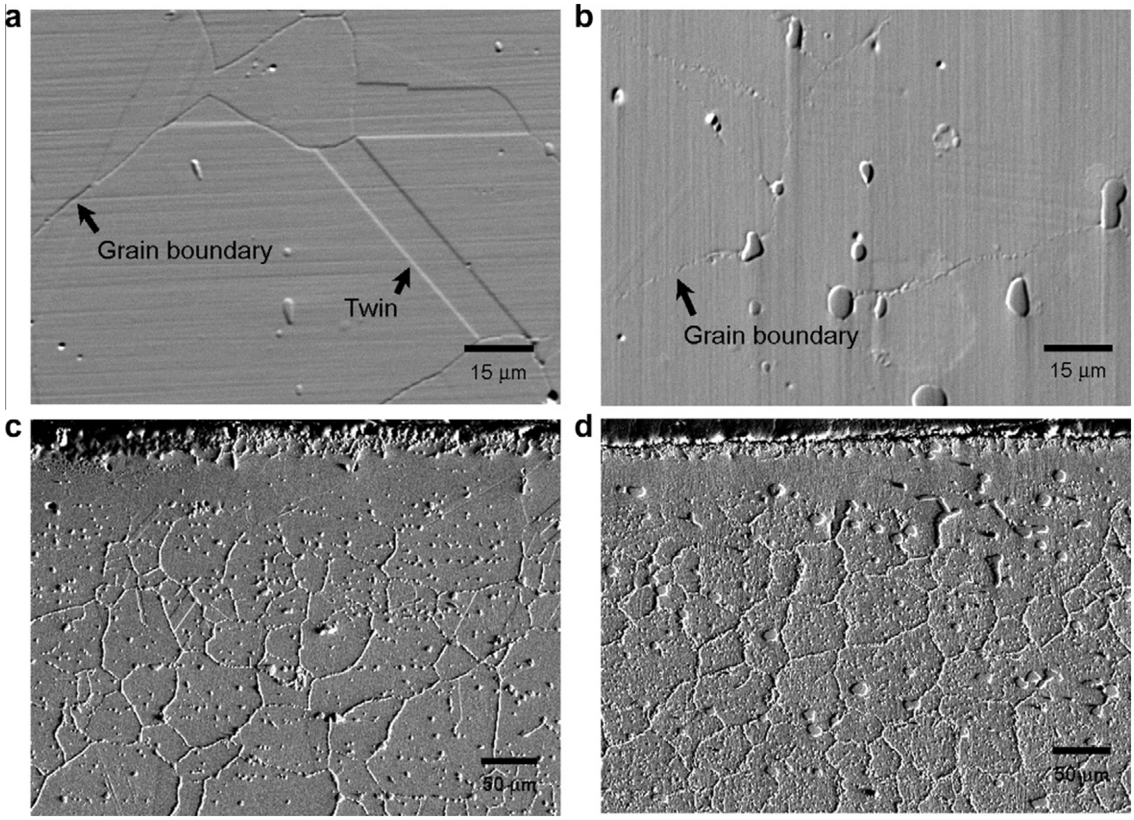

Fig. 3. Comparison of the carbide distribution in as-received condition: (a) Alloy 617, (b) Haynes 230, and after 500 h exposure in impure helium, (c) Alloy 617 and (d) Haynes 230.

bides was extensive below the carbide-free zone, which suggested that the carbon dissolved in the matrix could have contributed to the thermodynamic growth of carbides during high temperature exposure.

3.2. Tensile behaviors

Fig. 4 shows tensile test results of Alloy 617 and Haynes 230 aged at 1000 °C in impure helium environment. A significant decrease in the elongation was observed as the aging progressed. For Alloy 617, elongation continuously decreased after short exposure time. On the other hand, for Haynes 230, elongation remained largely unchanged until 100 h of exposure, and then sharply decreased for the specimens aged for 500 h. The causes of the different behaviors will be discussed in the following section in view of the microstructural features. Compared to the reduction in elongation, the changes in yield strength and tensile strength were relatively small.

3.3. Fracture behavior of aged Alloy 617

Alloy 617 contains 1.1 wt.% Al, as shown in Table 1, to improve the oxidation resistance at high temperature. However, Al was not partitioned into the surface oxide layer when Alloy 617 was

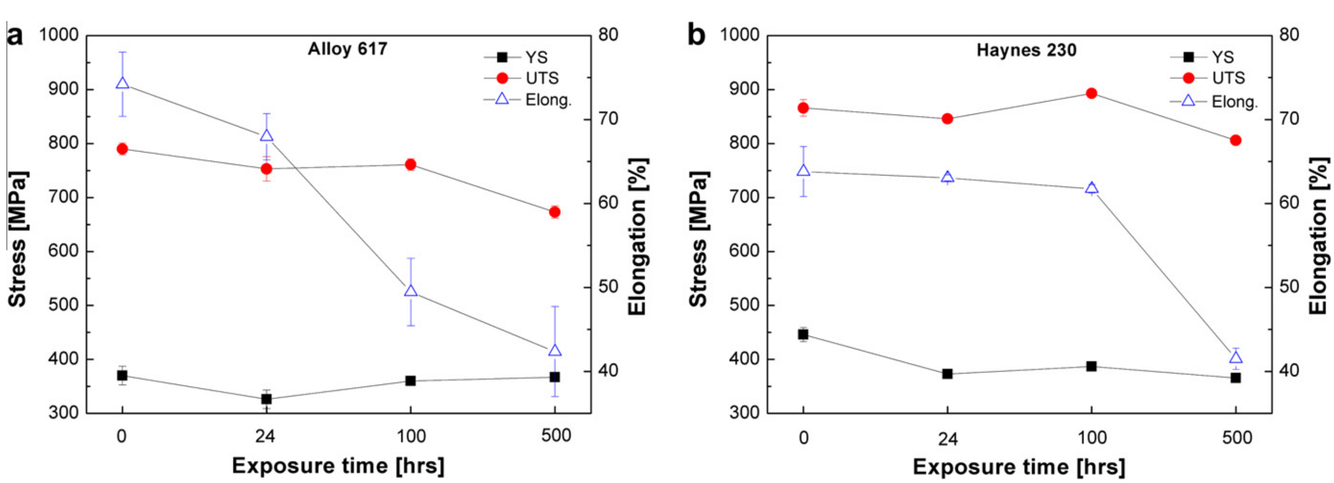

Fig. 4. Tensile property changes after being aged at 1000 °C in the impure helium environment: (a) Alloy 617 and (b) Haynes 230.

exposed in oxidizing environment at VHTR relevant temperatures. Instead, internal oxides were extensively developed as the finger-shaped Al_2O_3 islands along grain boundary under the chrome rich oxide layer, thus called as inter-granular oxidation [13]. The growth of inter-granular oxide islands were observed at very early stage of aging for Alloy 617. During tensile creep test of Alloy 617 in high temperature air, inter-granular oxide islands were developed and acted as preferential sites for surface cracks [16]. Similar behavior was observed in room temperature tensile test of aged specimen as shown in Fig. 5. In the figure, the inter-granular Al_2O_3 internal oxides were connected to the tip of the surface crack indicating that they were participating in cracking of aged Alloy 617 specimens.

As shown in Fig. 3a, there are wide region where thick and continuous carbides were formed on grain boundary below the carbide-free zone in the specimen aged for 500 h at 1000 °C. Some of those grain boundary carbides were cracked during the tensile test as shown in Fig. 6a. From the fracture surface shown in Fig. 6b, it is evident that grain boundaries are completely detached and the inter-granular cracking is extensive below the carbide-free zone. The inter-granular carbides were characterized using TEM. From the TEM diffraction patterns and corresponding EDS analysis results shown in Fig. 6c, grain boundary carbides of Alloy 617 were identified as $M_{23}C_6$ type, with M being Cr, Mo. Therefore, the loss of ductility for the aged Alloy 617 could be attributed to the inter-granular oxides and grain boundary carbides which are associated with inter-granular fracture.

3.4. Fracture behavior of aged Haynes 230

For aged Haynes 230, the internal oxidation was not extensive as shown in Fig. 7a and b, in part because of small amount of Al and protective oxide layer like $MnCr_2O_4$ on the surface [14]. Instead, large globular precipitates were dominantly formed near the carbide-free zone and in occasionally the environmentally not affected matrix as shown in the same figure after 500 h exposure at 1000 °C. It should be noted that they were not observed in the specimens aged for 100 h or less.

During tensile test, the localized brittle fracture occurred in the globular precipitates, but it was apart from the crack in the surface oxide layer as shown in Fig. 7a and b. In Fig. 7c, or the fracture surface near the surface, the fracture mode was a mixture of ductile and brittle, and faceted surface was mostly covered with fractured pieces of globular precipitates. The nature of the globular precipitates was characterized using TEM. As shown in Fig. 7d, TEM diffraction patterns well matched to $Cr_{0.8}Ni_{0.2}$ intermetallic with BCC structure, instead of M_xC_y type carbides which are common in superalloys like Haynes 230. Some papers have mentioned that

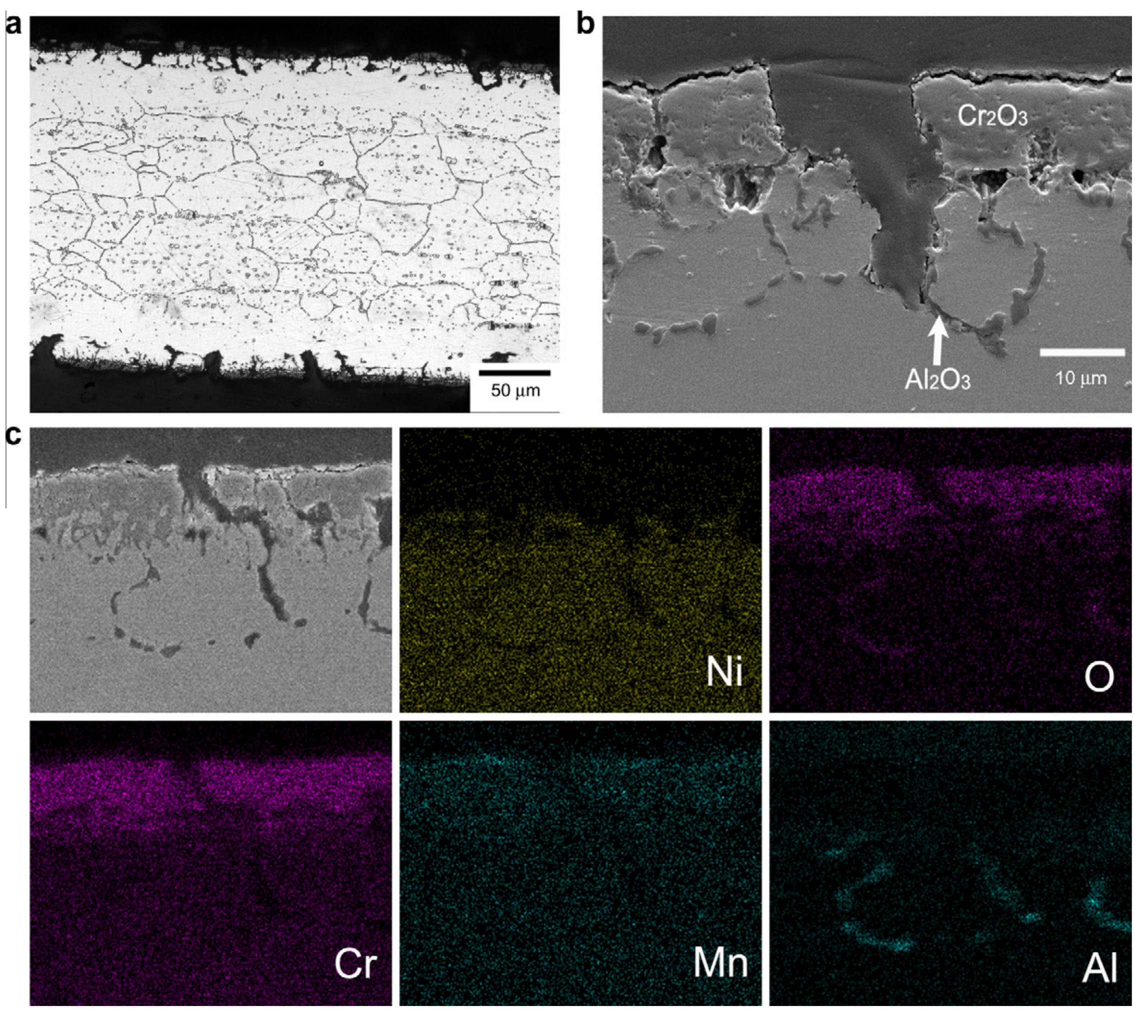

Fig. 5. Cracking along Al_2O_3 inter-granular oxides of Alloy 617 aged for 500 h in the impure helium environment at 1000 °C: (a) area away from the fracture region, (b) cross-sectional area at high magnification, (c) EDS mapping result.

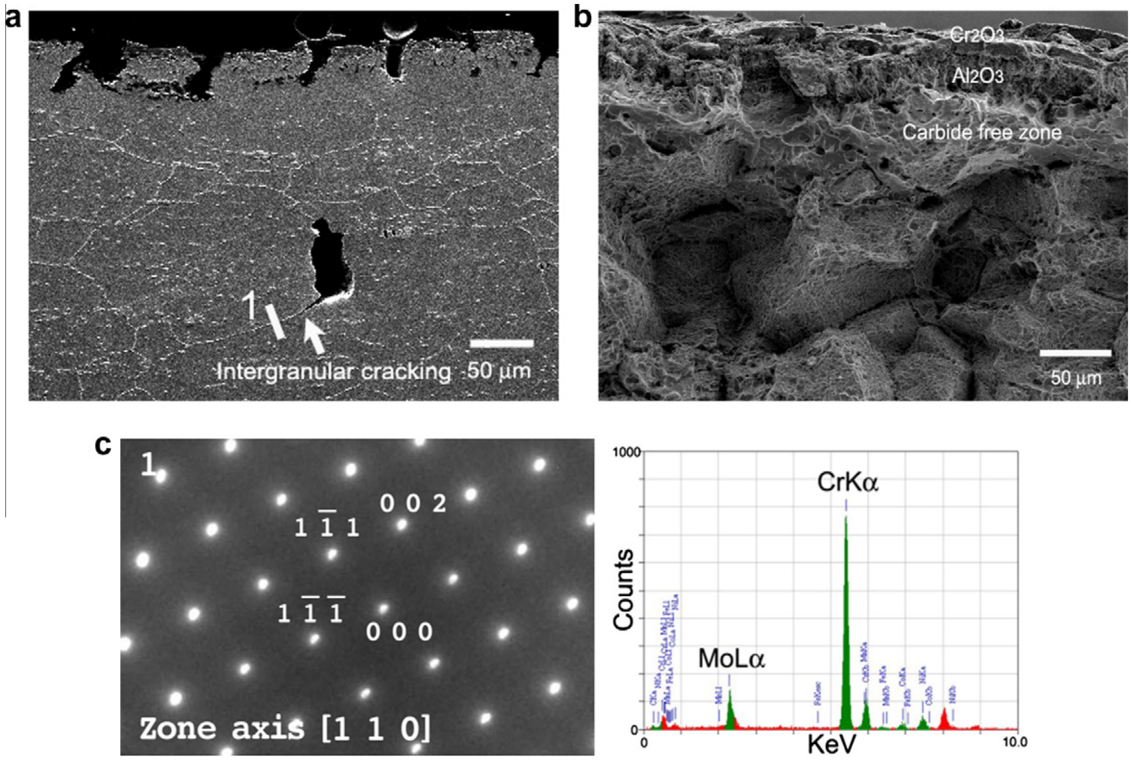

Elements	At%
C	10.5
Cr	73.0
Mn	0.2
Co	1.5
Ni	4.1
Mo	10.6

Fig. 6. Cracking along grain boundary carbides of Alloy 617 aged for 500 h in the impure helium environment at 1000 °C: (a) cross-sectional area, (b) fracture surface, (c) diffraction pattern and EDS peaks.

the globular precipitates are brittle and Cr-rich phases or carbides [17,18], but no carbon was detected by quantitative EDS analysis as shown in Fig. 7d. Therefore, it was thought that once the globular intermetallic precipitates were formed after long aging time, they contributed to cracking in the near surface region of aged Haynes 230 specimens during tensile test. This resulted in a significant loss of ductility after 500 h aging for Haynes 230.

Along with the large globular intermetallic precipitates, the medium-sized globular intra- and inter-granular carbides were grown during the aging treatment as shown in Fig. 3d. During tensile test, those globular carbides were preferentially fractured and it led to the localized brittle fracture as shown in Fig. 8a and b. Fracture surface is covered with a mixture of ductile dimples, isolated brittle facets, a local inter-granular crack surface, and fracture mode was also a mixture of inter-granular and intra-granular, which indicates that crack path was largely determined by the fracture of the globular and grain boundary carbides. From the TEM diffraction patterns and corresponding EDS analysis results shown in Fig. 8c and 8d, it was indicated that globular carbides with faceted morphology were identified as M_6C type, with M being W, Cr, and Ni. Grain boundary carbide was identified as $M_{23}C_6$, with M being mainly Cr. Despite the fracture of globular carbides during tensile test, its contribution to the loss of ductility was not so significant, as shown in Fig. 4b.

4. Conclusions

The effects of high temperature environmental damage on low temperature embrittlement of wrought nickel-base superalloys, such as Alloy 617 and Haynes 230 were evaluated. They were aged at 1000 °C in the impure helium containing 5.0 Pa CO, 1.0 Pa CO_2, <0.1 Pa CH_4, and 0.07 Pa H_2O up to 500 h. The effects of the inter-granular oxide and the coarsening of carbides on room temperature tensile properties were also examined. Based on the tensile test and analysis, the following conclusions were drawn:

(1) In both alloys, an oxidation region and a narrow carbide-free zone were formed after aged for 500 h as expected in helium environment with low CH_4 content. However, extensive growth of carbides was observed below the carbide-free zone.
(2) Loss of room temperature ductility was gradually increased for Alloy 617, while steep decrease in ductility was observed for Haynes 230 specimen aged for 500 h.
(3) For Alloy 617, Al_2O_3 inter-granular oxides below the surface oxide layer and the coarsening of carbides on the grain boundaries caused the gradual loss of ductility. For the same reason, the fracture mode was predominantly inter-granular.

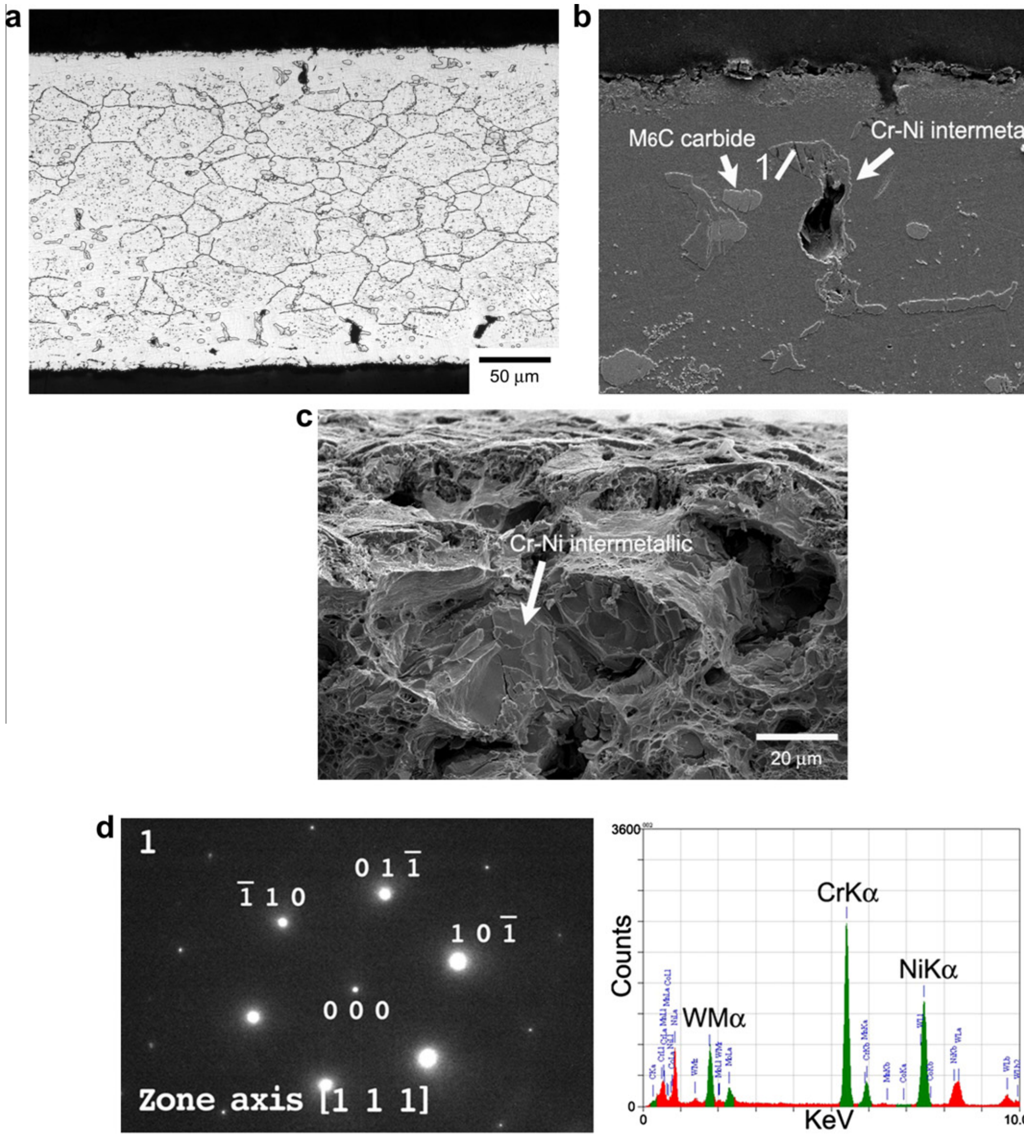

Elements	At%
C	0
Cr	50.8
Mn	1.2
Co	0.4
Ni	36.5
Mo	5.1
W	5.9

Fig. 7. Cracking along intermetallic precipitates of Haynes 230 aged for 500 h in the impure helium environment at 1000 °C: (a) area away from the fracture region, (b) cross-sectioned area at low and high magnification, (c) fracture surface, (d) diffraction pattern and EDS peaks.

(4) The significant loss of ductility in Haynes 230 was only observed after 500 h of aging when the large intermetallic precipitates were extensively formed and brittle inter-granular cracking began to occur.

(5) Fracture mode of Haynes 230 was influenced by the fracture of globular carbides in grains and grain boundaries as well as brittle intermetallic precipitates, resulting in the mixed mode of inter-granular and intra-granular fracture.

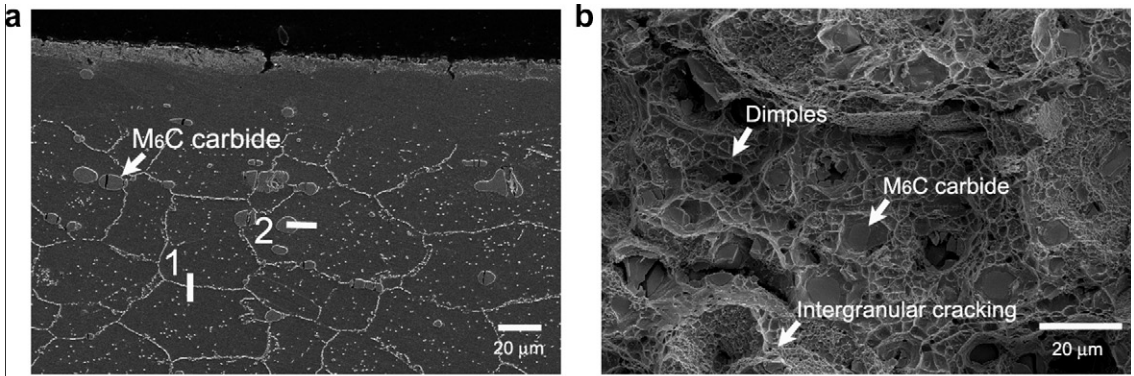

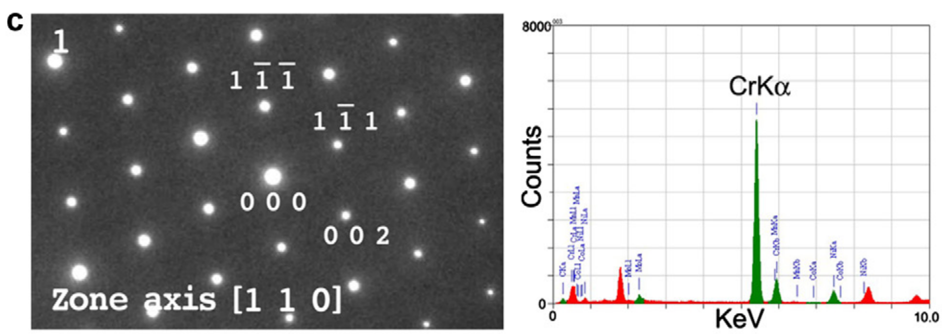

Elements	At%
C	10.2
Cr	78.8
Mn	2.2
Ni	5.6
Mo	3.1

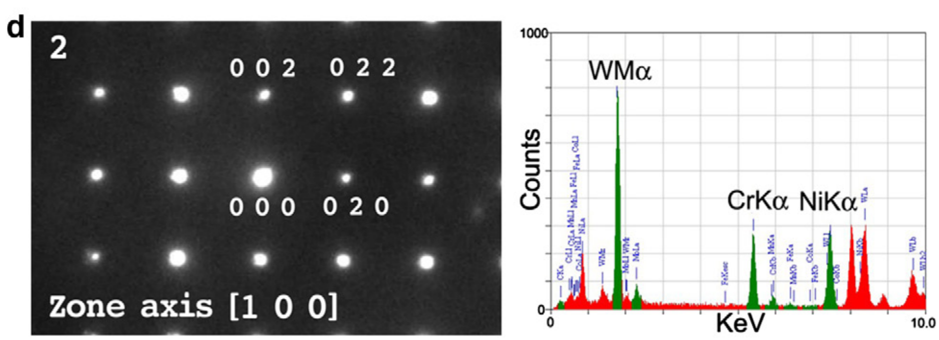

Elements	At%
C	10.0
Cr	23.7
Mn	0.5
Co	0.8
Ni	29.2
Mo	6.2
W	29.1

Fig. 8. Inter-granular cracking and micro-cracking in large globular carbides of Haynes 230 aged in the impure helium environment after 500 h exposure at 1000 °C: (a) cross-sectioned area, (b) fracture surface, (c) diffraction pattern and EDS peaks of particle 1 in (a), and (d) diffraction pattern and EDS peaks of particle 2 in (a).

Acknowledgements

This work was supported by the MEST/NRF (Nuclear R&D Program, 2005-2004718 and 2009-0083392) of Korea. Part of the funding was provided by the Second Phase BK21 Program of the Ministry of Education, Science and Technology of Korea.

References

[1] W.R. Corwin et al., Generation IV Reactors Integrated Materials Technology Program Plan: Focus on Very High Temperature Reactor Materials, ORNL/TM-2008/129, 2008.
[2] R.N. Wright, Kinetics of Gas Reactions and Environmental Degradation in NGNP Helium, INL/EXT-06-11494, 2006.
[3] R. Nieder, W. Stroter, VGB Kraftwerstechnik 68 (1988) 671–676.
[4] R. Nieder, Prediction on an HTR Coolant Composition After Operational Experience with Experimental Reactors, Specialists Meeting on Coolant Chemistry, Plate-out and Decontamination in Gas Cooled Reactors, International Working Group on Gas-Cooled Reactors IWGGCR-2 December 2–4, 1980, Juelich, Germany.
[5] H.J. Christ, U. Kunecke, K. Meyer, H.G. Sockel, Materials Science and Engineering 87 (1987) 161–168.
[6] H.J. Christ, U. Kunecke, K. Meyer, H.G. Sockel, Oxidation of Metals 30 (1/2) (1988).
[7] L.W. Graham, Journal of Nuclear Materials 171 (1990) 76–83.
[8] C. Cabet, F. Rouillard, Journal of Nuclear Materials 392 (2009) 235–242.
[9] NGNP with Hydrogen Production IHX and Secondary Heat Transport Loop Alternatives, AREVA Report, Document No. 12-9076325-001, 2008.
[10] R. Wright, J. Simpson, A. Wertsching, W.D. Swank, High temperature behavior of candidate VHTR heat exchanger alloys, in: Proceedings of the 4th International Topical Meeting on High Temperature Reactor Technology HTR2008 September 28–October 1, 2008, Washington, DC, USA.
[11] D. Lee, D. Kim, C. Jang, Oxidation characteristics of nickel-base superalloys at high temperature in air and helium atmospheres, in: Proceedings of the International Conference on Advanced Power Plant ICAPP'07, May 13–18, 2007, Nice, France.
[12] C. Cabet, J. Chapovaloff, F. Rouillard, G. Girardin, D. Kaczorowski, K. Wolski, M. Pijolat, Journal of Nuclear Materials 375 (2008) 173–184.
[13] D. Kim, C. Jang, W.S. Ryu, Oxidation of Metals 71 (2009) 271–293.
[14] W.J. Quadakkers, H. Schuster, Werkstoffe und Korrosion 36 (1985) 141–150.
[15] T. Hirano, H. Aiuki, H. Yosida, Journal of Nuclear Materials 97 (1981) 272–280.
[16] C. Jang, D. Lee, D. Kim, International Journal of Pressure Vessels and Piping 85/6 (2008) 368–377.
[17] H. Burlet, J.M. Gentzbittel, P. Lamagnere, C. Cabet, M. Blat, D. Renaud, S. Dubiez-Le Goff, D. Pierron, Evaluation of nickel-base materials for VHTR heat exchanger, in: Structural Materials for Innovative Nuclear Systems (SMINS), OECD Publishing, London, 2008.
[18] J. Veverkova, A. Strang, G.R. Marchant, G.M. McColvin, H.V. Atkinson, High temperature microstructural degradation of Haynes Alloy 230, in: Proceeding of Superalloys 2008, September 14–18 2008, Champion, PA USA.